THE JOURNAL OF PHYSICAL CHEMISTRY B

Article

Cite This: J. Phys. Chem. B 2018, 122, 2389−2395

pubs.acs.org/JPCB

Influence of Water on Carbon Dioxide and Room Temperature Ionic Liquid Dynamics: Supported Ionic Liquid Membrane vs the Bulk Liquid

Jae Yoon Shin, Steven A. Yamada, and Michael D. Fayer*

Department of Chemistry, Stanford University, Stanford, California 94305, United States

Supporting Information

ABSTRACT: The influence of water on the dynamics of a room temperature ionic liquid (RTIL), 1-ethyl-3-methylimidazolium bis(trifluoromethylsulfonyl)imide (EmimNTf$_2$), and CO_2 in the RTIL was studied in the bulk liquid and a supported ionic liquid membrane (SILM) using two-dimensional infrared (IR) and IR polarization selective pump−probe spectroscopies. In the water-saturated bulk EmimNTf$_2$, the complete orientational randomization and structural spectral diffusion (SSD) of CO_2 became faster than in the dry EmimNTf$_2$. In the poly(ether sulfone) SILM, only the longer time components of the SSD became faster in the water-saturated RTIL; the complete orientational randomization remained similar to the dry RTIL in the SILM. The implication is that the presence of water in EmimNTf$_2$ contained in the SILM facilitates the fluctuation of globally modified RTIL structure in the pores, but the local RTIL environments are relatively unaffected.

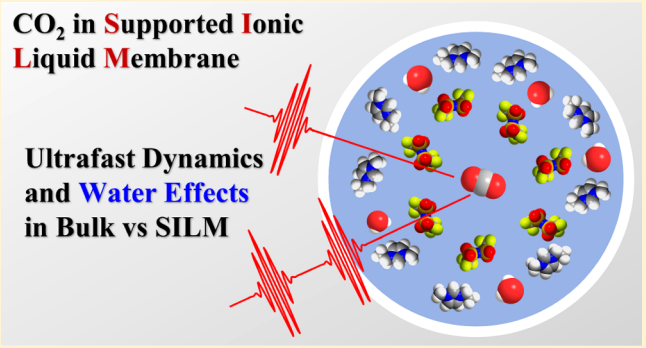

I. INTRODUCTION

Supported ionic liquid membranes (SILMs) are promising materials for CO_2 capture.[1−4] SILMs consist of organic or inorganic porous membranes impregnated with room temperature ionic liquids (RTILs) in the pores. Because of the large surface area per unit volume and their mechanical structure, SILMs can efficiently capture CO_2. Because CO_2 does not react with the RTIL, costly chemical regeneration is not necessary. CO_2 diffuses through the RTIL/membrane from the high CO_2 concentration side to exit on the low concentration side.[1−4] There have been many efforts to improve the SILM design and performance[1−4] since the first SILM study was reported in 2002.[5] Recently, we carried out polarization selective pump−probe (PSPP) and two-dimensional infrared (2D IR) experiments on poly(ether sulfone) (PES) SILMs prepared with 1-ethyl-3-methylimidazolium bis(trifluoromethylsulfonyl)imide (EmimNTf$_2$) under dry conditions.[6,7] In these studies, the orientational relaxation of $SeCN^-$ and CO_2 and the structural dynamics of the RTIL significantly slowed down in two SILMs compared to the bulk RTIL. This result was surprising, given the fact that the SILMs had large averaged pore sizes of ∼100 and ∼350 nm, indicating long-range modification of RTIL structures by interaction with the pore interfaces.[6,7] Time-dependent fluorescence Stokes shift measurements studying the effect of the RTIL cation alkyl chain length on the dynamics supported the results of the earlier work.[8]

In the postcombustion CO_2 capture, SILMs will be exposed to humid conditions where the gas can contain 10% water.[9] Therefore, the RTIL in the membrane pores will be saturated with water. Even though EmimNTf$_2$ is not highly hygroscopic, it picks up a non-negligible amount of water at saturation, up to a mole fraction of 0.278.[10] The presence of water can change the CO_2 and RTIL dynamics in SILMs, but the effects of water on SILMs' properties are not well understood.[11,12] For example, the viscosity of bulk RTILs generally decreases with the presence of water,[10,13] which can enhance CO_2 diffusivity. However, the water effect on the CO_2 diffusivity in SILMs may differ from that in the bulk RTIL because the mesoscopic RTIL structure and dynamics in SILMs are different from those in the bulk.[6−8] To this end, the current study examined the influence of water on the CO_2 and RTIL dynamics by comparing the PSPP and 2D IR experimental results for bulk and PES200 membrane samples with an average pore size of ∼350 nm[6] prepared with dry and water-saturated EmimNTf$_2$.

II. EXPERIMENTAL METHODS

II.I. Sample Preparation. EmimNTf$_2$ was purchased from Iolitec and stored in a nitrogen glovebox after drying under vacuum (∼100 mTorr) at ∼65 °C. Isotopically labeled $^{13}CO_2$ (<99% isotopic purity) and poly(ether sulfone) membrane (Supor 200) were purchased from Icon Isotopes and Pall corporation, respectively. The water-saturated EmimNTf$_2$ was prepared by extracting EmimNTf$_2$ from the phase-separated water−EmimNTf$_2$ mixture that was stirred overnight after the

Received: February 1, 2018
Published: February 7, 2018

DOI: 10.1021/acs.jpcb.8b01163
J. Phys. Chem. B 2018, 122, 2389−2395

addition of water. The SILM samples containing $^{13}CO_2$ were prepared according to previously described procedure,[7] except that the water-saturated $EmimNTf_2$ was used for making the wet SILM samples. Water absorption bands in Fourier transform infrared (FT-IR) spectrum confirmed that the water content in the RTIL of the wet bulk and SILM samples were nearly the same.

II.II. Time-Resolved Ultrafast Infrared Experiments. The details of the experimental setup are described in the Supporting Information, and only a brief outline is presented here. A Ti:sapphire regenerative amplifier pumped a home-built optical parametric amplifier creating mid-IR pulses centered at 2277 cm^{-1} with ~6 μJ pulse energy. The mid-IR beam was split into two beams, a stronger pump pulse and a weaker probe pulse. The pump pulse was passed through an acousto-optic mid-IR Fourier-domain pulse shaper. In the PSPP experiments, the pulse shaper choped the pump pulse to obtain transient absorption signals, whereas in the 2D IR experiments the pulse shaper generated two excitation pulses and controlled the delay time (τ) between them. In addition, the pulse shaper controlled the phase of the pulses and was used to overcome light scattering, which was the major difficulty in performing the laser experiments on the membranes. A mechanical delay stage in the probe pulse path controlled the time delay between the pump and probe pulses in the PSPP experiments or the time delay (waiting time, T_w) between the second excitation pulse and the third excitation pulse (probe pulse) in the 2D IR experiments. The pump and probe pulses are focused into the sample with a small crossing angle for both experiments.

After passing through the sample, the probe pulse was directed into a spectrograph. The spectrograph dispersed the probe pulse, which was then detected in the frequency domain by a 32 pixel HgCdTe (MCT) IR array detector. The 2D IR signal was collinear with the third pulse (probe pulse), which also acted as the local oscillator used for heterodyne detection of the signal. In the PSPP measurements, the probe polarization was horizontal (in the plane of the optical table) and the pump polarization was at 45° with respect to the probe pulse. After the sample, a polarizer mounted on a computer controlled rotation stage alternately resolved the probe pulse at +45° (parallel to the pump) and −45° (perpendicular to the pump) relative to the incident polarization (horizontal). Because the response of the spectrograph grating depended on polarization, another horizontal polarizer was placed in front of the spectrometer's entrance slit to ensure that there was no bias in the detection of the polarizations. To carry out the polarization selective 2D IR measurements, the polarization of both excitation pulses was set to 0 or 90° relative to the probe polarization (horizontal) in the ⟨*XXXX*⟩ (parallel) and ⟨*XXYY*⟩ (perpendicular) configurations, respectively, using a half-wave-plate followed by a polarizer. The resolving polarizer after the sample was fixed to horizontal and not changed for either polarization configurations.

III. RESULTS AND DISCUSSION

III.I. Linear IR Absorption Spectra. Figure 1 displays the FT-IR absorption spectra of $^{13}CO_2$ in the bulk RTIL and the SILM under both dry and water-saturated conditions. As shown in Figure 1A, the asymmetric stretch band of $^{13}CO_2$ in the bulk RTIL appears at 2276 cm^{-1}.[14] The water saturated bulk RTIL has an identical $^{13}CO_2$ absorption spectrum within the experimental error (Figure 1A).

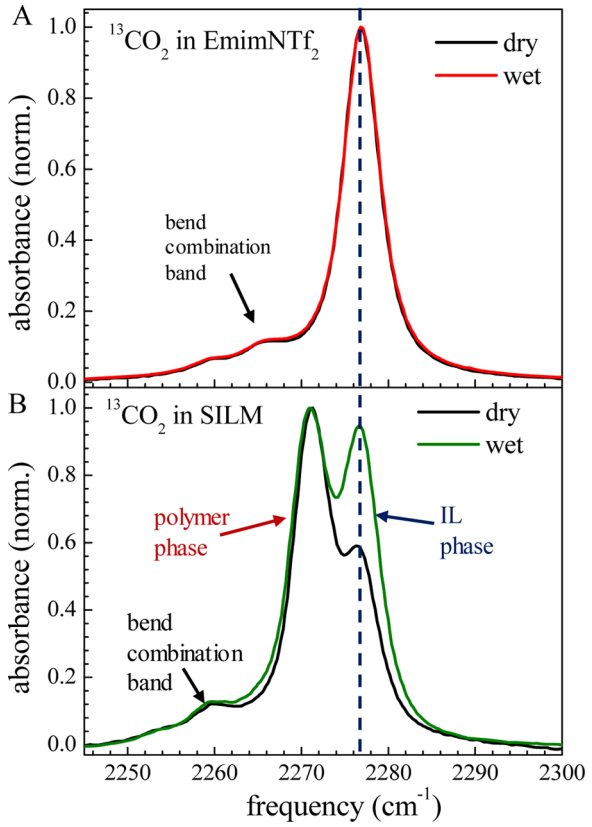

Figure 1. Background-subtracted FT-IR spectra of $^{13}CO_2$ in (A) dry and wet bulk $EmimNTf_2$ and (B) SILMs prepared with dry and wet $EmimNTf_2$.

The absorption spectrum of $^{13}CO_2$ in the SILM (Figure 1B) has an additional peak along with the 2276 cm^{-1} bulk peak. In the SILM, the CO_2 resides in the RTIL/pores and in the PES membrane material. The band at 2271 cm^{-1} was previously assigned to the asymmetric stretch of CO_2 in the polymer.[7] $^{13}CO_2$ in the polymer is isolated from the RTIL/pores and, thus, behaves differently; CO_2's orientational relaxation and spectral diffusion in the polymer are much slower than they are in the RTIL/pores.[7] Water in the RTIL/pores does not affect CO_2 in the polymer; the results presented here focus on CO_2 in the RTIL/pores.

The water in the RTIL in the SILM changes the relative amplitudes of the asymmetric stretch band of CO_2 in the RTIL/pores and in the polymer, whereas the band positions do not change (see Figure 1B). CO_2 is added to the wet and dry samples in an identical manner. The membranes containing RTIL or RTIL/water in the pores are placed in 2 mL vials under CO_2 pressure of ~0.123 atm, which is 200 times the quantity of CO_2 necessary to saturate the RTIL in the SILM with CO_2 based on the bulk solubility. (The CO_2 solubility in the bulk $EmimNTf_2$ has been reported to be 0.1 $mol{\cdot}L^{-1}{\cdot}atm^{-1}$ and the same with and without water in $EmimNTf_2$.[12]) Typically, the samples are kept in the CO_2 atmosphere for 20 min, but tests at 1 and 10 h do not change the band ratios. Because of the difficulty of measuring the absolute absorbance of the samples due to the extreme light scattering through the membranes, only the ratio of the two peak amplitudes can be reliably determined. Preparation of many different dry and wet samples shows that the band ratios are reproducible. The increase in the relative size of the CO_2 band in the RTIL/pores

DOI: 10.1021/acs.jpcb.8b01163
J. Phys. Chem. B 2018, 122, 2389−2395

with water compared to the CO_2 in the polymer suggests that CO_2 is more soluble when the RTIL is saturated with water than when it is dry. As discussed later, the time-dependent measurements show that the dynamics are different in the wet and dry membrane samples, which in turn differ from the bulk wet and dry RTILs.

The linear absorption spectra are sensitive to the structures and interactions of CO_2 with the local surrounding environment. The absence of change in the absorption spectrum of CO_2 in the RTIL with water indicates that the environment surrounding CO_2 is little changed by the addition of water. Water and CO_2 do not have strong attractive interactions as evidenced by the low CO_2 solubility in water; the CO_2 in the wet RTIL samples apparently avoids direct interactions with water and will mostly interact with the anions of the RTIL.

III.II. PSPP Measurements: Population and Rotational Dynamics. Vibrational relaxation is affected by interactions of the vibrational chromophore with the surrounding solvent molecules. In general, the vibrational energy in the initially excited mode flows into the combinations of intramolecular lower frequency modes and the continuum of low frequency intermolecular bath modes during relaxation.[15] Therefore, the vibrational lifetime is sensitive to the environment of a vibrational oscillator. The vibrational lifetime of the $^{13}CO_2$ asymmetric stretch band in dry EmimNTf$_2$ is measured to be 64 ± 2 ps.[14] The decay constant in the dry SILM sample is 61 ± 2 ps.[7] These values are the same within experimental error. The vibrational lifetimes of the same band for the wet RTIL samples are obtained in this study as previously described in the dry RTIL studies.[7] The time constant is 59 ± 1 ps for both wet bulk and SILM samples. The wet samples give almost the same lifetimes as those in the dry samples. The results indicate a small change in lifetimes in the wet samples compared to the corresponding dry samples, but the error bars overlap. The absorption spectra (Figure 1) show no significant effects with the addition of water, indicating little change in the interactions of CO_2 with its surroundings. The lifetime measurements show at most a small influence of water on the local interactions of CO_2 with the RTIL/water mixture.

Anisotropy decays (orientational relaxation) change substantially in the wet samples. Figure 2 presents the anisotropy decays of CO_2 in the RTIL bulk and SILM samples. The anisotropy consistently decays faster when the RTIL contains water in both the bulk and SILM samples. For the bulk, the anisotropy decay curves are fit well with triexponentials. The triexponential decays arise from short time restricted angular sampling of CO_2 followed by the complete randomization on the longest time scale. The data can be interpreted with the wobbling-in-a-cone model.[16,17]

The anisotropy decays in the SILM also can be fit with triexponentials. The PES membrane has a large pore size distribution that ranges from 100 to 500 nm (see inset Figure 2).[6] A previous study of two PES membranes with different average pore sizes showed that the dynamics are strongly dependent on the pore sizes, slowing for smaller pores.[6] Therefore, CO_2 in the different pore sizes of PES200 will have different dynamics. The results for the SILMs are averages over a distribution of orientational relaxation times. For an initial comparison, we will use the correlation time, τ_{cor}, which is the integral of the curves. The correlation times are obtained by integrating the triexponential fits to normalized anisotropy decay data. The normalized orientational relaxation correlation function (second Legendre correlation function) fit parameters

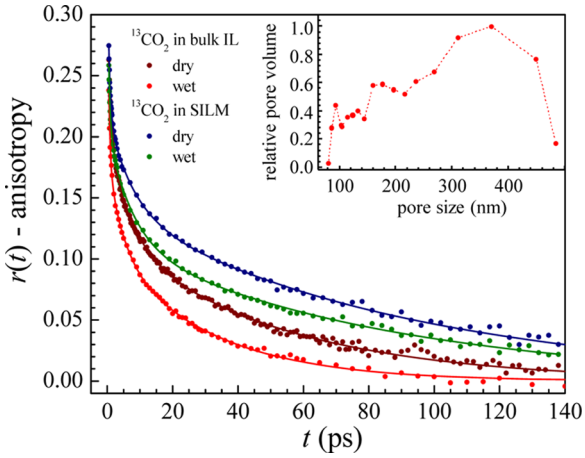

Figure 2. Anisotropy decay curves of $^{13}CO_2$ in the bulk EmimNTf$_2$ and SILM under dry and wet conditions. The solid curves are triexponential fits to the data. The data for the dry samples were reproduced from ref 7. The inset shows the broad distribution of relative membrane pore volumes vs pore size, which was reproduced from ref 6.

are given in the Supporting Information (Table S1). For the bulk samples, the correlation times are 22 ps (dry) and 11 ps (wet). In the SILMs, the correlation times are 38 ps (dry) and 30 ps (wet). As can be seen in Figure 2 and from the correlation times, saturating the RTIL with water causes the orientational relaxation to become faster. For both dry and wet samples, the orientational relaxation in the SILMs is slower than that in the bulk liquid. The change in going from dry to wet is greater in the bulk liquid than in the SILM.

Although the anisotropy decays obtained for SILMs are an average over pore sizes, the fact that they are described well with triexponential functions indicates that the CO_2 orientational dynamics occur in the same manner as in bulk samples. The three time constants found for the SILM samples are the times for wobbling and complete orientational relaxation, but each process is still an averaged observable over the distribution of pore sizes. Nonetheless, it is still useful to compare the time constants and amplitudes of the exponentials and to perform the wobbling-in-a-cone analysis (Table 1). The analysis enables us to acquire the time for the complete orientational diffusion of CO_2 in the SILM. The rotational diffusion is closely related to the translational diffusion that is an important measure of SILM performance. (In addition, the parameters from the wobbling-in-a-cone analysis are used in the 2D IR data analysis as discussed later.)

All of the curves show initial anisotropy values less than 0.4 (the maximum anisotropy, see Figure 2). CO_2 undergoes inertial motions, responsible for the initial drop from 0.4, on an ultrafast time scale that cannot be resolved in the experiments. In the wobbling model, the CO_2 can sample a limited range of angles, a cone, determined by the constraints imposed by the solvation environment. Relaxation of the constraints on some time scale allows a larger range of angles to be sampled until additional constraints are released. Eventually, the CO_2 will be able to sample all of the angles, i.e., complete orientational randomization. The triexponential decays indicate that the two cones are sampled diffusively, followed by complete diffusive randomization. In addition, there is an initial inertial cone. From the wobbling-in-a-cone analysis,[18−21] the triexponential decay time constants and the associated amplitudes yield the

DOI: 10.1021/acs.jpcb.8b01163
J. Phys. Chem. B 2018, 122, 2389−2395

Table 1. Parameters from Wobbling Analysis

sample		θ_{in} (deg)[a]	θ_{c1} (deg)[b]	θ_{c2} (deg)[b]	θ_{tot} (deg)[c]	τ_{c1} (ps)[d]	τ_{c2} (ps)[d]	τ_{m} (ps)[d]	D_{c1} (10^{-2} ps^{-1})[e]	D_{c2} (10^{-2} ps^{-1})[e]
bulk	dry[f]	22.5 ± 1.5	30.3 ± 0.9	33.3 ± 0.8	48.7 ± 0.5	0.9 ± 0.1	7.4 ± 0.9	52 ± 1	8.2 ± 1.4	1.2 ± 0.1
	wet	16.3 ± 3.4	36.9 ± 1.4	33.1 ± 0.9	50.5 ± 0.6	0.5 ± 0.1	5.6 ± 0.9	31 ± 1	21.6 ± 3.6	1.6 ± 0.3
SILM	dry[f]	16.6 ± 2.7	31.5 ± 1.3	30.4 ± 0.7	45.5 ± 0.4	0.6 ± 0.1	8.2 ± 1.1	90 ± 2	12.9 ± 2.3	0.9 ± 0.1
	wet	17.2 ± 2.0	33.0 ± 0.9	35.1 ± 0.4	49.5 ± 0.3	0.5 ± 0.1	8.2 ± 0.6	84 ± 2	16.1 ± 2.0	1.2 ± 0.1

[a]The inertial cone angle. [b]θ_{c1} and θ_{c2} are the first and second diffusive cone half angles, respectively. [c]The total cone half angle accounting for all three cones. [d]τ_{c1}, τ_{c2}, and τ_{m} are the decay times associated with the first and second diffusive cones and the final free diffusion, respectively. [e]D_{c1} and D_{c2} are the first and second cone diffusion constants, respectively. [f]Numbers are from ref 7.

half-cone angles, θ_i, the wobbling time constants, τ_{c1} and τ_{c2}, and the final complete orientational relaxation time constant, τ_m. For complete orientational relaxation, the orientational diffusion constant is $D_m = 1/6\tau_m$. However, the cone diffusion constants are determined both by the time constants and the cone angles.[18−21] The cone diffusion constants, D_{c1} and D_{c2}, are given in Table 1.

The bulk half-cone angles of the inertial and second diffusive cones are similar for dry and wet conditions within the error bars, whereas the first diffusive cone angle increases in the wet sample. Both cone diffusion constants increase (diffusion is faster), although there is a larger difference for D_{c1}. The complete orientational relaxation time constant, τ_m, becomes faster in the wet bulk sample by a factor of ∼1.7. This facilitated reorientation of CO_2 in the wet bulk sample is in the direction of the decrease in the viscosity of $EmimNTf_2$ upon addition of water. Saturation of $EmimNTf_2$ with water reduces the viscosity from 36.3 to 18.2 cP.[10] The optical heterodyne-detected optical Kerr effect measurements of the bulk dynamics of $EmimNTf_2$ show that the complete orientational randomization of the liquid is hydrodynamic, and its time constant decreases upon water saturation by a factor of 2.[10] However, it is also found that the complete orientational diffusion of CO_2 in the RTILs does not quite track the decrease in viscosity.[16] Thus, the 1.7-fold decrease in τ_m in the wet bulk sample reflects the decrease in the effective viscosity near CO_2, not the change in the bulk viscosity.

The half-cone angles and wobbling time constants for both dry and wet SILM samples do not largely differ from those for the bulk samples. Both cone diffusion constants slightly increase in the wet SILM compared to the dry SILM. However, τ_m is substantially slower in the dry SILM than in the dry bulk liquid. In addition, the change in τ_m with water-saturated RTIL in the SILM is smaller than in the bulk; the reorientation only becomes ∼7% faster. The slowdown of τ_m in the dry SILM compared to the dry bulk sample was previously attributed to the modification of the RTIL structure induced by the pore interface that propagates a long distance from the pore wall, that is the long range RTIL ordering effect.[6,7] The small change in τ_m of the wet SILM compared to the dry membrane suggests that this long-range RTIL ordering still exists in the membrane pore when the RTIL contains water, and the local environment and the local viscosity experienced by CO_2 are changed little upon the addition of water.

III.III. Two-Dimensional IR Measurements: Spectral Diffusion and Structural Dynamics. Two-dimensional IR spectroscopy reports on the structural dynamics of liquids via measurement of spectral diffusion of a vibrational probe molecule.[22,23] In a 2D IR experiment, the first two IR pulses in the pulse sequence in effect label the vibrational probe molecules with their initial frequencies across the inhomogeneously broadened absorption line. Structural dynamics of the liquid cause the intermolecular interactions with the probe to change, and, therefore, the frequencies of the probe molecules to evolve. After a waiting time, T_w, the third pulse in the sequence induces the emission of the vibrational echo (fourth pulse) from the sample. The vibrational echo reads out the vibrational probe frequencies after the period T_w. Two Fourier transforms are performed on the time domain data to yield a 2D IR spectrum. Two-dimensional spectra are acquired for a range of T_w. As T_w increases, the liquid structure has more time to evolve, and the shape of the 2D spectrum changes. Measurement of the time evolution of the 2D spectral shape is the measurement of the structural evolution of the liquid. The time evolution of the 2D line shape is quantified by the frequency−frequency correlation function (FFCF).[24,25] The center-line-slope (CLS) method is used to obtain the normalized FFCF from a series of 2D IR spectra measured as a function of T_w.[24,25]

Figure 3 displays the CLS decay curves for CO_2 in bulk and SILM samples measured under dry and wet RTIL conditions.

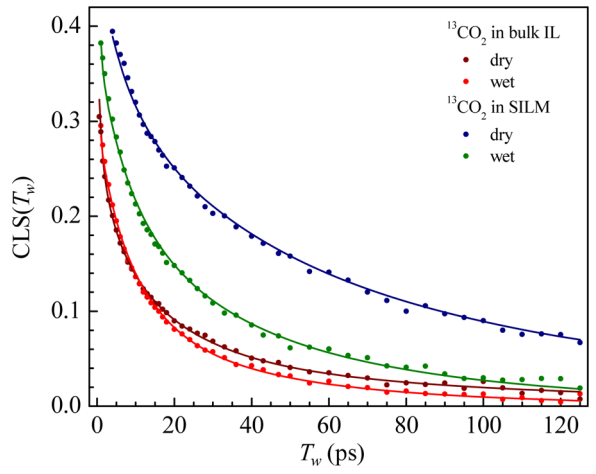

Figure 3. Two-dimensional IR CLS (normalized frequency−frequency correlation function) decay data for the asymmetric stretch of $^{13}CO_2$ in the bulk $EmimNTf_2$ and SILM from the perpendicular polarization configuration ($\langle XXYY \rangle$). The solid curves are the second-order reorientation-induced spectral diffusion (RISD) fits to the data. The data for the dry samples were reproduced from ref 7.

These data are taken with perpendicular polarizations, that is, pulses 1 and 2 have vertical polarization, whereas pulse 3 and the vibrational echo have a horizontal polarization ($\langle XXYY \rangle$). The use of perpendicular and parallel polarization 2D IR experiments is discussed later. In Figure 3, both the bulk and SILM samples' CLS curves measured under the wet condition decay faster than those of the dry samples. Before analyzing the data in detail, the correlation times, τ_{cor}^{2D}, are discussed. As with the anisotropy decays, τ_{cor}^{2D} were calculated by integrating the

DOI: 10.1021/acs.jpcb.8b01163
J. Phys. Chem. B 2018, 122, 2389−2395

Table 2. SSD Parameters from RISD Fits Based on the Second-Order Stark Effect Model

sample		scalar				vector	
		A_1[a]	τ_1 (ps)	A_2[a]	τ_2 (ps)	A_3[a]	τ_3 (ps)
bulk	dry[b]	0.09 ± 0.02	20 ± 5	0.07 ± 0.02	77 ± 20	0.36 ± 0.01	57 ± 5
	wet	0.13 ± 0.01	10 ± 1	0.09 ± 0.01	50 ± 3	0.22 ± 0.01	47 ± 4
SILM	dry[b]	0.04 ± 0.01	17 ± 8	0.17 ± 0.01	143 ± 11	0.54 ± 0.01	113 ± 7
	wet	0.07 ± 0.02	16 ± 3	0.11 ± 0.02	72 ± 9	0.44 ± 0.01	58 ± 4

[a]Amplitude of each exponential. [b]Values are from ref 7.

Table 3. Ratios of Fit Parameters among Dry/Wet and SILM/Bulk Samples

sample		anisotropy	SSD		
		τ_m	τ_1	τ_2	τ_3
dry/wet	bulk	1.65 ± 0.06	2 ± 0.54	1.54 ± 0.41	1.21 ± 0.15
	SILM	1.08 ± 0.04	1.06 ± 0.54	1.99 ± 0.29	1.95 ± 0.18
SILM/bulk	dry	1.76 ± 0.05	0.85 ± 0.45	1.86 ± 0.50	1.98 ± 0.21
	wet	2.68 ± 0.11	1.6 ± 0.34	1.44 ± 0.20	1.23 ± 0.14

curves using exponential fits to the data. For the bulk samples, τ_{cor}^{2D} equals 21.7 ps and 17.9 ps for dry and wet samples, respectively. For the membrane samples, τ_{cor}^{2D} equals 54.5 and 31.0 ps for dry and wet samples, respectively. Saturating the RTIL with water has a larger effect on the dynamics of the SILM than it does on the dynamics of the bulk liquid. This is evident by inspecting Figure 3 and confirmed by the correlation times. For the SILM samples, the wet membrane displays RTIL dynamics that are 1.75 times faster than that in the dry membrane. The ratio is only 1.2 for the bulk samples.

In addition to the structural dynamics of the liquid, the rotation of the probe molecule itself can contribute to spectral diffusion if the rotational time scale is comparable to the time scale of spectral diffusion. This is called reorientation-induced spectral diffusion (RISD), and polarization selective 2D IR measurements are necessary for extracting the structural spectral diffusion (SSD) from the combined structural and reorientation-induced spectral diffusion.[26,27] Therefore, the polarizations of the pulses are controlled to be all of the same, i.e., parallel ($\langle XXXX \rangle$) or, as mentioned above, perpendicular ($\langle XXYY \rangle$). The RISD model, which is previously developed based on the second-order Stark effect for CO_2 and other molecules that do not have a dipole moment difference upon excitation,[16] is utilized in the data fit. (See the Supporting Information for details of the experiment and theory.)

Using the measured orientational relaxation data, the SSD parameters are obtained from the fits to the CLS data.[16] The results are summarized in Table 2. The second-order Stark-RISD model separates CO_2 SSD into contributions from scalar and vector interactions with the RTIL.[16] For CO_2 in the bulk RTILs and the RTILs in the pores of the SILMs, a biexponential scalar term and a single exponential vector term give the best fits to the experimental CLS decays.[7,16] In the dry RTIL condition, the longer time constant of the scalar term, τ_2, and the vector time constant, τ_3, become significantly slower in the SILM compared to the bulk, whereas the shorter time constant of the scalar term, τ_1, is unchanged within the experimental error (Table 2). It is suggested that the slowdown in the longer time constants of SSD reflects the change in the global RTIL structure and dynamics and is consistent with the long-range RTIL structuring induced by the pore interfaces.[7] The shortest time constants likely reflect very local structural fluctuations, which, like the spectrum (Figure 1), are unchanged in going from the bulk to the membrane. When the RTIL is saturated with water, the SSD is accelerated in both bulk and SILM samples; the time constants of the SSD decrease in the wet RTIL condition for both samples, with the exception of the SILM shortest time constant, τ_1 (Table 2). However, the extent of change induced by water differs between the bulk and SILM. This difference is shown clearly in the correlation times, τ_{cor}^{2D}, given earlier in the paper.

III.IV. Water Effects on the Dynamics in the SILM. The ratios of the SSD time constants and the complete reorientational diffusion time constant, τ_m, are given in Table 3 and Figure 4. Figure 4A presents the ratios of the time constants of the dry sample to those from the wet sample and compares the trends for the bulk and SILM samples. It shows that all four time constants of the bulk sample are affected by water, with the dynamics accelerated upon addition of water. In contrast, for the SILM samples, water only impacts the longer time scale SSD parameters, τ_2 and τ_3, whereas the complete orientational diffusion, τ_m, and the short time SSD, τ_1, remain basically unchanged. Moreover, the ratios of τ_2 and τ_3 for the SILM are larger than those for the bulk. When the time constant ratios are calculated for the SILM and bulk samples and compared between dry and wet conditions, as displayed in Figure 4B, the ratios of τ_2 and τ_3 become smaller in going from dry to wet conditions. However, the ratios of τ_m and τ_1 increase for the wet samples because these time constants for the SILMs are almost unaffected under wet condition but become significantly faster in the bulk RTIL.

As mentioned earlier, the longer time scale SSD parameters, τ_2 and τ_3, reflect the fluctuations of global RTIL structure, whereas the short time SSD and the complete orientational diffusion report on the local structural fluctuations. Therefore, the trend observed in the time constant ratios suggests that water facilitates the global fluctuations of liquid structure in the SILM more than it does in the bulk, but it does not greatly impact the local RTIL environments experienced by the CO_2 molecules in the SILM. In addition, the presence of water in the SILM does not seem to hamper the long-range RTIL structuring induced by the membrane interface; under wet condition, all of the ratios are larger than 1, meaning that the overall dynamics in the wet SILM are still slower than those in the wet bulk (see Figure 4B).

Finally, the results suggest that the diffusivity of CO_2 through the SILM used in this study will not be significantly improved by the presence of water. The orientational diffusion of CO_2 in

DOI: 10.1021/acs.jpcb.8b01163
J. Phys. Chem. B 2018, 122, 2389−2395

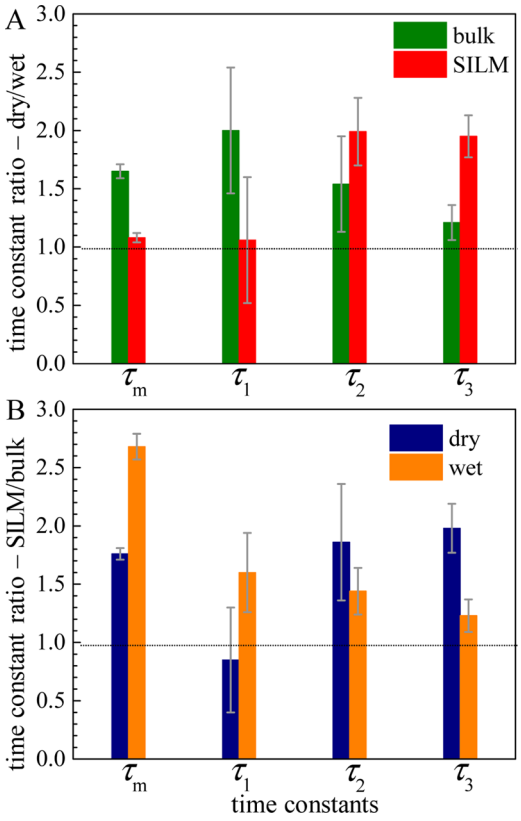

Figure 4. Ratios of time constants (A) between dry and wet and (B) between SILM and bulk samples. τ_m is the time constant for the complete orientational randomization of CO_2. The τ_i are the SSD parameters obtained from the second-order RISD fits.

the SILM is mainly governed by the local RTIL environment. Water only affects the global RTIL structural fluctuations in the SILM, but the local RTIL structures and, thus, the reorientation of CO_2 are relatively insensitive to the water content. If the orientational relaxation and the translational diffusion are consistent with hydrodynamics, then the complete orientational relaxation, τ_m, is given by the Debye–Stokes–Einstein equation and the translational diffusion is described by the Stokes–Einstein equation. These equations are closely related, suggesting that if the orientational diffusion is not affected by the addition of water, then the translational diffusion will also not be affected.[7] Indeed, Scovazzo et al. observed that the CO_2 permeability through the same SILM as used in the current study did not change significantly with the relative humidity of the gas.[12] (The permeability is the product of solubility and diffusivity in the solution–diffusion mass-transfer model.)[1−4] The permeability only increased from 960 to 1050 barrers as the relative humidity of CO_2 changes from 10 to 85%.[12] Figure 1B may suggest that CO_2 solubility increases somewhat in the wet SILM. Therefore, our results are consistent with those from the CO_2 permeability experiments of Scovazzo et al. On the other hand, Zhao et al. reported a different water effect on the CO_2 permeability in the SILM consisting of PES membranes and 1-butyl-3-methylimidazolium bis(trifluoromethylsulfonyl)-imide ($BmimBF_4$). In that SILM, the CO_2 permeability increases when the water content in the RTIL is small, but decreases again as the water content increases.[11] They attributed their observation to the combined effects of water, that is, enhancing diffusivity and diminishing solubility of CO_2; the diffusivity effect is more dominant at the low water content, but the solubility effect becomes predominant at the high water content.[11] It is important to note that $BmimBF_4$ is completely miscible with water, which can result in different water effects in the SILM. Therefore, similar water effects as those observed in the current study are expected in the SILMs containing other nonwater-miscible RTILs, and significant enhancement in CO_2 diffusion by the addition of water in these SILMs is unlikely.

IV. CONCLUDING REMARKS

The water effects on the CO_2 dynamics in the bulk $EmimNTf_2$ and SILM were investigated by the PSPP and 2D IR spectroscopies. The FT-IR spectrum of asymmetric stretch band of CO_2 in the water-saturated $EmimNTf_2$ did not differ from that measured in the dry condition. In the wet SILM sample, the relative size of CO_2 band in the RTIL/pores increased compared to the CO_2 band in the PES polymer without the frequency shifts or band broadening. This may indicate the change in CO_2 solubility in the wet SILM. The vibrational lifetimes of CO_2 band were very similar between wet and dry samples for both bulk and SILM samples. Unchanged absorption spectrum and vibrational lifetimes were indicative of the negligible influence of water on the local interaction of CO_2 with its surroundings. Anisotropy decays from the PSPP measurements and CLS decays from the 2D IR experiments demonstrated that water effects on the CO_2 and RTIL dynamics were different between the bulk and SILM samples. In the bulk samples, the time constants for the complete orientational diffusion of CO_2, τ_m, and the SSD time constants decreased by a factor of 1.2−2 as $EmimNTf_2$ was saturated with water and the effective viscosity was decreased (Table 3 and Figure 4A). In contrast, only the longer time scale SSD parameters, τ_2 and τ_3, decreased by a factor of 2 in the wet SILM sample, whereas τ_m and the short time scale SSD, τ_1, remained unchanged (Table 3 and Figure 4A). These results suggested that in the SILM, water accelerated the global fluctuations of ordered RTIL structures but did not affect the local RTIL environments near CO_2 molecules. Because the orientational diffusion process is strongly related to the translational diffusion that is an important measure of the SILM performance for CO_2 capture, the results implied that the translational diffusion of CO_2 would not be improved by the addition of water in the SILM prepared with nonwater-miscible RTILs like $EmimNTf_2$.

■ ASSOCIATED CONTENT

Supporting Information

The Supporting Information is available free of charge on the ACS Publications website at DOI: 10.1021/acs.jpcb.8b01163.

Detailed descriptions of experimental methods and second-order Stark effect RISD theory, triexponential fit parameters of anisotropy decays, CLS decay curves for parallel ($\langle XXXX \rangle$) polarization configuration, and isotropic FFCF parameters (PDF)

■ AUTHOR INFORMATION

Corresponding Author

*E-mail: fayer@stanford.edu. Phone: 650 723-4446.

ORCID

Michael D. Fayer: 0000-0002-0021-1815

Notes

The authors declare no competing financial interest.

DOI: 10.1021/acs.jpcb.8b01163
J. Phys. Chem. B 2018, 122, 2389−2395

■ ACKNOWLEDGMENTS

This work was funded by the Division of Chemical Sciences, Geosciences, and Biosciences, Office of Basic Energy Sciences of the U.S. Department of Energy through Grant No. DE-FG03-84ER13251. Additional support of the equipment and partial support of S.A.Y. were provided by the Air Force Office of Scientific Research Grant No. FA9550-16-1-0104. S.A.Y. acknowledges the support from a Stanford Graduate Fellowship.

■ REFERENCES

(1) Tomé, L. C.; Marrucho, I. M. Ionic Liquid-Based Materials: A Platform to Design Engineered CO_2 Separation Membranes. *Chem. Soc. Rev.* **2016**, *45*, 2785−2824.
(2) Zeng, S.; Zhang, X.; Bai, L.; Zhang, X.; Wang, H.; Wang, J.; Bao, D.; Li, M.; Liu, X.; Zhang, S. Ionic-Liquid-Based CO_2 Capture Systems: Structure, Interaction and Process. *Chem. Rev.* **2017**, *117*, 9625−9673.
(3) Wang, J.; Luo, J.; Feng, S.; Li, H.; Wan, Y.; Zhang, X. Recent Development of Ionic Liquid Membranes. *Green Energy Environ.* **2016**, *1*, 43−61.
(4) Lozano, L. J.; Godínez, C.; de los Ríos, A. P.; Hernández-Fernández, F. J.; Sánchez-Segado, S.; Alguacil, F. J. Recent Advances in Supported Ionic Liquid Membrane Technology. *J. Membr. Sci.* **2011**, *376*, 1−14.
(5) Scovazzo, P.; Visser, A. E.; Davis, J. H.; Rogers, R. D.; Koval, C. A.; DuBois, D. L.; Noble, R. D. Supported Ionic Liquid Membranes and Facilitated Ionic Liquid Membranes. In *Ionic Liquids*; American Chemical Society: Washington, DC, 2002; Vol. *818*, pp 69−87.
(6) Shin, J. Y.; Yamada, S. A.; Fayer, M. D. Dynamics of a Room Temperature Ionic Liquid in Supported Ionic Liquid Membranes vs the Bulk Liquid: 2D IR and Polarized IR Pump-Probe Experiments. *J. Am. Chem. Soc.* **2017**, *139*, 311−323.
(7) Shin, J. Y.; Yamada, S. A.; Fayer, M. D. Carbon Dioxide in a Supported Ionic Liquid Membrane: Structural and Rotational Dynamics Measured with 2D IR and Pump-Probe Experiments. *J. Am. Chem. Soc.* **2017**, *139*, 11222−11232.
(8) Thomaz, J. E.; Bailey, H. E.; Fayer, M. D. The Influence of Mesoscopic Confinement on the Dynamics of Imidazolium-Based Room Temperature Ionic Liquids in Polyether Sulfone Membranes. *J. Chem. Phys.* **2017**, *147*, No. 194502.
(9) Kenarsari, S. D.; Yang, D.; Jiang, G.; Zhang, S.; Wang, J.; Russell, A. G.; Wei, Q.; Fan, M. Review of Recent Advances in Carbon Dioxide Separation and Capture. *RSC Adv.* **2013**, *3*, 22739−22773.
(10) Bailey, H. E.; Wang, Y.-L.; Fayer, M. D. Impact of Hydrogen Bonding on the Dynamics and Structure of Protic Ionic Liquid/Water Binary Mixtures. *J. Phys. Chem. B* **2017**, *121*, 8564−8576.
(11) Zhao, W.; He, G.; Zhang, L.; Ju, J.; Dou, H.; Nie, F.; Li, C.; Liu, H. Effect of Water in Ionic Liquid on the Separation Performance of Supported Ionic Liquid Membrane for CO_2/N_2. *J. Membr. Sci.* **2010**, *350*, 279−285.
(12) Scovazzo, P.; Kieft, J.; Finan, D. A.; Koval, C.; DuBois, D.; Noble, R. Gas Separations Using Non-Hexafluorophosphate $[PF_6]^-$ Anion Supported Ionic Liquid Membranes. *J. Membr. Sci.* **2004**, *238*, 57−63.
(13) Seddon, K. R.; Stark, A.; Torres, M.-J. Influence of Chloride, Water, and Organic Solvents on the Physical Properties of Ionic Liquids. *Pure Appl. Chem.* **2000**, *72*, No. 2275.
(14) Giammanco, C. H.; Kramer, P. L.; Yamada, S. A.; Nishida, J.; Tamimi, A.; Fayer, M. D. Coupling of Carbon Dioxide Stretch and Bend Vibrations Reveals Thermal Population Dynamics in an Ionic Liquid. *J. Phys. Chem. B* **2016**, *120*, 549−556.
(15) Kenkre, V.; Tokmakoff, A.; Fayer, M. Theory of Vibrational Relaxation of Polyatomic Molecules in Liquids. *J. Chem. Phys.* **1994**, *101*, 10618−10629.
(16) Giammanco, C. H.; Kramer, P. L.; Yamada, S. A.; Nishida, J.; Tamimi, A.; Fayer, M. D. Carbon Dioxide in an Ionic Liquid: Structural and Rotational Dynamics. *J. Chem. Phys.* **2016**, *144*, No. 104506.
(17) Giammanco, C. H.; Yamada, S. A.; Kramer, P. L.; Tamimi, A.; Fayer, M. D. Structural and Rotational Dynamics of Carbon Dioxide in 1-Alkyl-3-methylimidazolium Bis(trifluoromethylsulfonyl)imide Ionic Liquids: The Effect of Chain Length. *J. Phys. Chem. B* **2016**, *120*, 6698−6711.
(18) Lipari, G.; Szabo, A. Effect of Librational Motion on Fluorescence Depolarization and Nuclear Magnetic Resonance Relaxation in Macromolecules and Membranes. *Biophys. J.* **1980**, *30*, 489−506.
(19) Wang, C.; Pecora, R. Time-Correlation Functions for Restricted Rotational Diffusion. *J. Chem. Phys.* **1980**, *72*, 5333−5340.
(20) Tan, H.-S.; Piletic, I. R.; Fayer, M. D. Orientational Dynamics of Water Confined on a Nanometer Length Scale in Reverse Micelles. *J. Chem. Phys.* **2005**, *122*, No. 174501.
(21) Kramer, P. L.; Giammanco, C. H.; Fayer, M. D. Dynamics of Water, Methanol, and Ethanol in a Room Temperature Ionic Liquid. *J. Chem. Phys.* **2015**, *142*, No. 212408.
(22) Park, S.; Kwak, K.; Fayer, M. D. Ultrafast 2D-IR Vibrational Echo Spectroscopy: A Probe of Molecular Dynamics. *Laser Phys. Lett.* **2007**, *4*, 704.
(23) Zheng, J.; Kwak, K.; Fayer, M. D. Ultrafast 2D IR Vibrational Echo Spectroscopy. *Acc. Chem. Res.* **2007**, *40*, 75−83.
(24) Kwak, K.; Park, S.; Finkelstein, I. J.; Fayer, M. D. Frequency-Frequency Correlation Functions and Apodization in Two-Dimensional Infrared Vibrational Echo Spectroscopy: A New Approach. *J. Chem. Phys.* **2007**, *127*, No. 124503.
(25) Kwak, K.; Rosenfeld, D. E.; Fayer, M. D. Taking Apart the Two-Dimensional Infrared Vibrational Echo Spectra: More Information and Elimination of Distortions. *J. Chem. Phys.* **2008**, *128*, No. 204505.
(26) Kramer, P. L.; Nishida, J.; Fayer, M. D. Separation of Experimental 2D IR Frequency-Frequency Correlation Functions into Structural and Reorientation-Induced Contributions. *J. Chem. Phys.* **2015**, *143*, No. 124505.
(27) Kramer, P. L.; Nishida, J.; Giammanco, C. H.; Tamimi, A.; Fayer, M. D. Observation and Theory of Reorientation-Induced Spectral Diffusion in Polarization-Selective 2D IR Spectroscopy. *J. Chem. Phys.* **2015**, *142*, No. 184505.

DOI: 10.1021/acs.jpcb.8b01163
J. Phys. Chem. B 2018, 122, 2389−2395